Occurrence and robustness of current reversals in overdamped deterministic ratchets under symmetric forcing

R. Salgado-García,[1,2,*] G. Martínez-Mekler,[2] and M. Aldana[2]

[1]*Facultad de Ciencias, Universidad Autónoma del Estado de Morelos, Avenida Universidad 1001, Colonia Chamilpa, Caixa Postal 62210, Cuernavaca, Morelos, Mexico*

[2]*Instituto de Ciencias Físicas, Universidad Nacional Autónoma de México, Caixa Postal 62251, Apartado Postal 48-3, Cuernavaca, Morelos, Mexico*

(Received 8 April 2008; published 29 July 2008)

We analyze the conditions for the existence of current reversals in overdamped deterministic tilting ratchets under symmetric forcing. To this end, we use and extend the formalism recently introduced in R. Salgado-García, M. Aldana, and G. Martínez-Mekler [Phys. Rev. Lett. **96**, 134101 (2006)] to transform the equations of motion of the ratchet into discrete circle maps. For a periodic dichotomous forcing we show that the phenomenon of current reversal is not uncommon and exists for a nonzero measure set of the parameter space. Additionally, we show numerically that, for a wide class of ratchet potentials, current reversals also occur when the discontinuous dichotomous forcing is replaced by symmetric continuous driving forces. The likelihood of the occurrence of current reversals is a consequence of the structural stability under small perturbations of the associated circle map with rational rotation number.

DOI: 10.1103/PhysRevE.78.011126 PACS number(s): 05.60.Cd, 05.45.−a

I. INTRODUCTION

Current reversal (CR) in tilting ratchets has been the subject of numerous studies and has been used to model many different situations such as particle separation, intracellular transport, Josephson junction transport, etc. [1]. The role of noise outside the adiabatic limit [2], inertial effects [3–6], the interplay between temporal and spatial symmetries [7,8], the effects of colored noise or correlated nonequilibrium fluctuations [9–13], and interparticle interactions [14–16] are only a few examples of extensions of Magnasco's original model [17] that presented to CR in tilting ratchets. In particular for the case in which inertial effects are present both noise induced CRs [2,18] as well as deterministic CRs [4] have been extensively studied. Nonetheless, the overdamped regimen has been scarcely explored. To our knowledge, only one example has been put forward in Ref. [18], where CR is originated from a particular external forcing, namely, a trichotomous driving force taking the values $\{F_0,0,-F_0\}$.

In a recent paper [19] we have introduced an approach to analyze the dynamical properties of overdamped tilting ratchets, which consists in formally transforming the continuous equations of motion of the ratchet into discrete circle maps. This approach allows us to relate, in a formal way, the ratchet's current with the rotation number of the corresponding map. In doing so, well-known properties of the rotation number of circle maps can be used to understand behaviors, such as "current quantization" [2], the occurrence of Devil's staircases and the existence of current reversals [18,19]. Furthermore, it is also possible to show that CR can actually be observed for a wide class of ratchet potentials under a symmetric dichotomous driving. We provide a simple analytical criterion to predict when in such systems a ratchet potential will exhibit CR as a function of the external forcing amplitude. Another consequence of this approach is that we exhibit the existence of asymmetric ratchet potentials that do not lead to current rectification. In other words, the asymmetry in the ratchet potential is only a necessary (but not a sufficient) condition for current rectification to exist.

This result complements previous findings which specify symmetry properties that lead to zero current [1,20,21]. The symmetries considered therein are sufficient conditions for the current to vanish, but not necessary [19].

In this paper we give an in-depth detailed explanation of the results introduced in Ref. [19] on the connection between deterministic ratchets and circle maps, and extend the CR examples to more general cases. This analytic study, supported by numerical evidence, reveals that CR occurs for a wide range of parameter values. In fact, the regions of the parameter space in which CR exists are identified with Arnold-tongue structures of zero rotation number. Furthermore, we also show numerically that some of the potentials considered here preserve the CR when the external driving becomes a continuous symmetric forcing. This robustness of the CR under changes in the parameters, and even in the nature of the forcing (from dichotomous to continuous), is most likely due to the stability of rational rotation numbers under small changes in the circle map associated with the ratchet potential.

This paper is organized as follows. In Sec. II we present the working model and show, via a stroboscopic sampling of the overdamped tilting ratchet trajectories, that they are ruled by a circle map. In Sec. III we obtain the circle map associated to a particle with a square-wave external driving. In Sec. IV we derive the null current condition in a rigorous way. In Sec. V we establish the criterion for the existence of CR in terms of the expression for the ratchet's mean velocity in the adiabatic limit. As an example we consider a piecewise ratchet potential with four free parameters. We show for this model that the zones of CR in the parameter space are of nonzero measure and hence of common occurrence. We

*r.salgado.garcia@gmail.com

identify these zones with Arnold-tongue structures of zero rotation number. In Sec. VI we consider the dynamics of a particle in a piecewise linear ratchet potential under the action of a continuous symmetric forcing. In this case an appropriate choice of the potential leads to CR. Finally in Sec. VII we give a brief discussion of our results and state the main conclusions of our study.

II. DETERMINISTIC RATCHETS AS CIRCLE MAPS

We consider the deterministic tilting ratchet model in the overdamped regime. It consists of a particle moving through a one dimensional potential $V(y)$, which is asymmetric and periodic with period L: $V(y+L)=V(y)$. Since inertia effects can be neglected in the overdamped regime, the equation of motion of the particle is

$$\gamma\frac{dy}{dt}=f(y)+F(t), \tag{1}$$

where γ is the friction coefficient (which we will set equal to one in the following), $f(y)=-\partial V(y)/\partial y$, and $F(t)$ is the external driving force. Although the external driving force can be any symmetric and periodic function, we obtain analytic results for the specific case in which $F(t)$ is a periodic dichotomous function given by

$$F(t)=\begin{cases}F_0 & \text{if} \quad t \bmod[T]<T/2,\\ -F_0 & \text{if} \quad t \bmod[T]\geq T/2.\end{cases} \tag{2}$$

This is a square-wave function with period T.

In Ref. [19] we have shown that a periodic stroboscopic sampling of the solutions of Eq. (1) with the driving force (2) defines an invertible and continuous circle map. This stroboscopic sampling is defined as follows. Let $x_0,x_1,x_2,\ldots,x_n,\ldots$ be the sequence of real numbers given by

$$x_n=y(nT), \quad n=0,1,2,\ldots, \tag{3}$$

where $y(t)$ is the solution of Eq. (1) with the initial condition $x_0=y(0)$ and T is the period of the driving force $F(t)$. We will call the sequence $\{x_n\}_{n=0}^{\infty}$ the stroboscopic sampling with period T of the continuous trajectory $y(t)$. We can think of this sequence as being generated by a map $R_T(x)$ such that

$$x_{n+1}=R_T(x_n). \tag{4}$$

In the next section we show that, for the specific form of $F(t)$ given in Eq. (2), the map $R_T(x)$ is a circle map. However, it turns out that for any periodic function $F(t)$, the stroboscopic sampling $\{x_n\}_{n=0}^{\infty}$ can always be generated by a circle-map homeomorphism. In other words, there always exists an invertible and continuous function $R_T:\mathbb{R}\to\mathbb{R}$, such that $x_{n+1}=R_T(x_n)$, and with the following properties. (i) R_T is a monotonically increasing function, with continuous inverse, whose domain and image are both $\mathbb{R}$. (ii) R_T satisfies the lift property $R_T(x+L)=R_T(x)+L$. (iii) R_T satisfies the group property $R_T\circ R_T=R_{2T}$. Any function satisfying the three properties listed above is a lift of the class of (invertible) circle homeomorphisms. In particular, the map $R_T(x)$ defined in Eq. (4) satisfies these properties because of the invariance of Eq. (1) under the spatial and temporal shifts $x\to x+L$ and $t\to t+T$, respectively. These translational symmetries are better expressed in terms of the solutions of the differential equation. Let $Y(t;y_0)$ be the general solution of Eq. (1) with the (arbitrary) initial condition $y_0=y(0)$. In Appendix A we show that $Y(t;y_0)$ satisfies the following properties: (I) $Y(t;y_0+L)=Y(t;y_0)+L$, (II) $Y(t+T;y_0)=Y(t;Y(T;y_0))$. In Appendix B we prove that properties (i), (ii), and (iii) follow from properties I and II. Thus, the latter two properties are the cornerstone of the link between deterministic overdamped tilting ratchets and circle maps.

III. CIRCLE MAPS FOR THE SQUARE-WAVE FORCING

Here we present in detail the calculation (sketched in Ref. [19]) showing that the map $R_T(x)$ is a circle map when the external driving $F(t)$ is the periodic dichotomous function given in Eq. (2). Let $\{\chi_m\}_{m=0}^{\infty}$ be the stroboscopic sampling with period $T/2$ of the continuous trajectory $y(t)$, namely,

$$\chi_m=y(mT/2), \quad m=0,1,2,\ldots.$$

Clearly, the sequences $\{x_n\}_{n=0}^{\infty}$ and $\{\chi_m\}_{m=0}^{\infty}$ are related through $x_n=\chi_{2n}$. During the time interval $0\leq t<T/2$ the external forcing acquires the constant value $F(t)=F_0$. Thus, starting from an initial condition $y(0)=x_0=\chi_0$, after a time $T/2$ the particle will be at the position $y(T/2)=\chi_1$, which is implicitly given by

$$\int_{x_0}^{\chi_1}\frac{dy}{f(y)+F_0}=\frac{T}{2}. \tag{5}$$

Now we define the parameter τ_+ and the function $h_+(x)$ as

$$\tau_+=\int_0^L\frac{dy}{f(y)+F_0}, \tag{6a}$$

$$h_+(x)=\frac{L}{\tau_+}\int_0^x\frac{dy}{f(y)+F_0}. \tag{6b}$$

Note that τ_+ is just the time it would take for the particle to travel a spatial period L if it were only driven by the constant force F_0. Note also that for τ_+ and $h_+(x)$ to be well defined, it is necessary that $F_0>|\min\{f(y)\}|$. Under such circumstances, $h_+(x)$ is a continuous increasing function with continuous inverse and such that $h_+(x+L)=h_+(x)+L$. Denoting as h_+^{-1} the inverse of h_+, Eq. (5) can be solved for χ_1, which gives

$$\chi_1=h_+^{(-1)}(h_+(\chi_0)+\alpha_+), \tag{7}$$

where

$$\alpha_+=\frac{LT}{2\tau_+}. \tag{8}$$

At time $t=T/2$ the particle's position is χ_1 and the driving force changes to $-F_0$. Therefore, the position χ_2 of the particle at $t=T$ is given by the implicit equation

$$\int_{\chi_1}^{\chi_2}\frac{dy}{f(y)-F_0}=\frac{T}{2}. \tag{9}$$

Defining τ_- and $h_-(x)$ as in Eqs. (5), but with F_0 replaced by $-F_0$,

$$\tau_- = \int_0^L \frac{dy}{f(y) - F_0}, \tag{10a}$$

$$h_-(x) = \frac{L}{\tau_+} \int_0^x \frac{dy}{f(y) - F_0}, \tag{10b}$$

Eq. (9) can be formally solved for χ_2, obtaining

$$\chi_2 = h_-^{(-1)}[h_-(\chi_1) + \alpha_-], \tag{11}$$

where

$$\alpha_- = \frac{LT}{2\tau_-}. \tag{12}$$

Again, τ_- is the time it would take the particle to travel an entire spatial period L if only the force $-F_0$ were acting on it. Note that in order for τ_-, $h_-(x)$ and the inverse function h_-^{-1} to be well defined, F_0 must satisfy $F_0 > \max\{f(y)\}$. With this condition, $h_-(x)$ also satisfies $h_-(x+L) = h_-(x) + L$.

Finally, we define the functions $M_+(x)$ and $M_-(x)$ as

$$M_+(x) = h_+^{(-1)}[h_+(x) + \alpha_+], \tag{13a}$$

$$M_-(x) = h_-^{(-1)}[h_-(x) + \alpha_-]. \tag{13b}$$

With this definition, Eqs. (7) and (11) can be written in a simple way as

$$\chi_1 = M_+(\chi_0) \tag{14}$$

and

$$\chi_2 = M_-(\chi_1), \tag{15}$$

respectively. Taking into account that $x_n = \chi_{2n}$, the above is equivalent to $x_1 = (M_- \circ M_+)(x_0)$. Iterating this process over time, we obtain that the sequence $x_0, x_1, \ldots, x_n, \ldots$, is generated by

$$x_{n+1} = (M_- \circ M_+)(x_n) \equiv R_T(x_n). \tag{16}$$

We should point out that when the external forcing amplitude F_0 is below the thresholds $\max\{f(y)\}$ or $|\min\{f(y)\}|$, the maps M_+ and M_- can still be defined in terms of an implicit function. In such a case M_+ and M_- are no longer maps topologically conjugated to simple rotations. Rather, they become only invertible circle maps with fixed points located at the roots of $f(y) \pm F_0$. This can be seen if we note that $f(y) + F_0$ is the total force that moves the particle from a point ξ to another point ξ' located at the right of ξ. In terms of the map M_+ this is expressed as $\xi' = M_+(\xi)$. However, if the initial position of the particle is precisely the place at which the net force is zero, i.e., at some ξ^* for which $f(\xi^*) + F_0 = 0$, then the particle does not undergo any displacement and will remain in its positions until the positive pulse of $F(t)$ ends. This implies that M_+ satisfies the fixed point equation $\xi^* = M_+(\xi^*)$. A similar argument leads to the existence of fixed points for M_- when $f(y) - F_0 = 0$ has solutions.

IV. THE NULL CURRENT CONDITION

One of the most important quantities in ratchet systems is the flux of particles J. If we consider an ensemble of N noninteracting particles, each obeying Eq. (1), we can define the flux of particles as

$$J = \frac{1}{L}\frac{1}{N}\langle \sum_{i=0}^{N} \bar{v}_i \rangle, \tag{17}$$

where the angular braces $\langle \cdots \rangle$ denote the average over initial conditions, and $\bar{v}_i$ is the mean velocity of the ith particle. Since the particles do not interact, they are statistically independent and equivalent. Therefore, all the particles have the same average velocity $\langle \bar{v}_i \rangle = \langle \bar{v} \rangle$, $\forall i$. Under such circumstances, the current J can be written simply as

$$J = \frac{1}{L}\langle \bar{v} \rangle.$$

For any particle that follows the trajectory $y(t)$, the mean velocity $\bar{v}$ is given by

$$\bar{v} = \lim_{t \to \infty} \frac{y(t) - y(0)}{t}. \tag{18}$$

Note that the last limit can be written in terms of the stroboscopic sampling $\{x_n\}_{n=0}^{\infty}$ as

$$\bar{v} = \lim_{n \to \infty} \frac{y(nT) - y(0)}{nT} = \lim_{n \to \infty} \frac{x_n - x_0}{nT}.$$

Therefore $\bar{v}$ is, up to a constant factor, the rotation number $\rho(R_T)$ of the map $R_T(x)$:

$$\bar{v} = \frac{\rho(R_T)}{T}. \tag{19}$$

It is clear that both the rotation number and the mean velocity are independent of the initial condition $x_0 = y(0)$. Therefore, $\langle \bar{v} \rangle = \bar{v}$. This enables us to write the particle flux as

$$J = \frac{\bar{v}}{L} = \frac{\rho(R_T)}{LT}. \tag{20}$$

From the above equation it follows that zero rotation number is equivalent to vanishing current. Since a zero rotation number corresponds to a fixed point of $R_T(x)$, the null-current condition for the ratchet is obtained by finding the fixed points of $R_T(x)$. In Ref. [19] we have shown that the rotation number of R_T is zero if and only if the equality

$$\int_0^L \sinh[uf(y)]dy = 0, \tag{21}$$

holds for all $u \in \mathbb{R}$. This condition was derived under the assumption that F_0 does not take values below $\max\{f(y)\}$ or $|\min\{f(y)\}|$. However, the condition given in Eq. (21) for the rotation number to be zero is actually valid in the whole parameter space. Indeed, in Appendix C we show that, if the above condition is satisfied, then the current J vanishes even if $F_0 < \max\{|f(y)|\}$. It is interesting to note that condition 21 is fulfilled by symmetric and supersymmetric potentials which, as shown in [20,21], are unable to produce a finite current. We recall that these symmetries are sufficient conditions for the current to be zero in overdamped tilting ratchets, but not necessary [19].

V. CURRENT REVERSALS IN RATCHET POTENTIALS UNDER PERIODIC DICHOTOMOUS FORCING

In Ref. [19] we have shown that there are ratchet potentials, with symmetric forcing, which are able to rectify motion in both directions depending on the values of the model parameters, such as the forcing amplitude. In this section we generalize that result by introducing a more general piecewise-linear potential that exhibits current reversal in a wide region of the parameter space.

We start our discussion by establishing a sufficient condition for the existence of current reversals. In Ref. [19] it was shown that, in the adiabatic limit $T\to\infty$, the mean velocity is given by

$$\bar{v}_\infty := \lim_{T\to\infty} \bar{v} = \frac{L}{2}\frac{\tau_+ + \tau_-}{\tau_-\tau_+}. \tag{22}$$

From this equation it is clear that the sign of the current in the adiabatic limit is determined by $\tau_+ + \tau_-$. (Note that $\tau_- < 0$ and $\tau_+ > 0$ in the region of the parameter space where τ_+ and τ_- are well defined, and therefore $\tau_+\tau_- < 0$ always.) On the other hand, the integral

$$G(u) := \int_0^L \sinh[uf(y)]dy \tag{23}$$

is related to $\tau_+ + \tau_-$ through a Laplace transform. Indeed, from Eqs. (6a) and (10a) we have

$$\begin{aligned}\tau_+ + \tau_- &= \int_0^L \left(\frac{1}{F_0 + f(y)} - \frac{1}{F_0 - f(y)}\right)dy \\ &= -2\int_0^L \int_0^\infty e^{-uF_0}\sinh[uf(y)]du\ dy \\ &= -2\int_0^\infty e^{-uF_0}G(u)du,\end{aligned} \tag{24}$$

where in the last step there is a change in the order of integration of the variables u and y.

It follows from Eqs. (22) and (24) that the sign of the mean velocity $\bar{v}_\infty$ at the adiabatic limit, and hence of the ratchet's current J in the same limit, depend on the sign of $G(u)$. In fact, it is possible to show that changes in the sign of $G(u)$ are associated with current reversals. This is a consequence of the following result.

Proposition 1. If there exists a unique value $u^* > 0$ such that $G(u)$ changes sign, then there exists a value $F_0^* > \max\{|f(x)|\}$ of the forcing amplitude for which $\bar{v}_\infty$ changes sign.

Although we have requested uniqueness of u^* in proposition 1, the validity of this statement can be extended to the case of any odd number of positive roots of $G(u)$. A sketch of the proof of proposition 1 is given in Appendix F [24]. Here, instead of presenting the this proof, we illustrate the validity of the above property for two particular examples: a piecewise linear potential and a continuously differentiable potential.

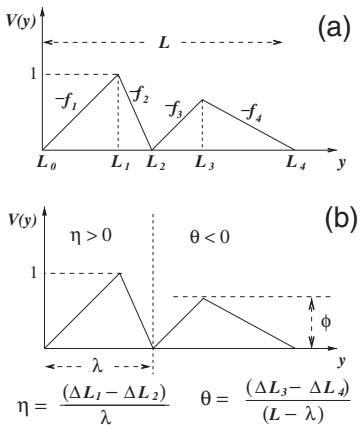

FIG. 1. Piecewise linear ratchet potential $V(y)$ with two peaks. (a) The set of points $\{0=L_0<L_1<L_2<L_3<L_4=L\}$ of the interval $[0,L]$ define a partition. The forces $\{f_1,f_2,f_3,f_4\}$ generated by the potential are minus the slopes of each element of the partition, are shown. (b) Geometrical meaning of the four free parameters $\{\phi,\lambda,\eta,\theta\}$ chosen to study the current reversal phenomenon. ϕ is the height of the right peak relative to the height of the left peak, λ is the length of the left peak, and η and θ, defined in terms of $\{\Delta L_i = L_i - L_{i-1}\}$, can be interpreted as quantities that measure the asymmetry of the left and right peaks, respectively. Note that $-\infty < \phi < \infty$, $0 \le \lambda < L$, and $-1 \le \eta, \theta < 1$.

Let $V(y)$ be the piecewise linear potential depicted in Fig. 1(a). This potential generates the steplike ratchet force $f(y)$ given by

$$f(y) = \begin{cases} f_1 & \text{if} \quad L_0 \le y \bmod[L] < L_1, \\ f_2 & \text{if} \quad L_1 \le y \bmod[L] < L_2, \\ f_3 & \text{if} \quad L_2 \le y \bmod[L] < L_3, \\ f_4 & \text{if} \quad L_3 \le y \bmod[L] < L_4, \end{cases} \tag{25}$$

where $\{L_0=0<L_1<L_2<L_3<L_4=L\}$ is an ordered set of points that defines a partition of the interval $[0,L)$. We define the quantities $\Delta L_i, i=1,2,3,4$ as the lengths of the intervals in this partition: $\{\Delta L_i = L_i - L_{i-1} \cdot i=1,2,3,4\}$. These lengths must satisfy that $\Sigma_{i=1}^4 \Delta L_i = L$. Therefore, only three out of these four quantities are independent. On the other hand, note that in order to generate the ratchet potential with two peaks shown in Fig. 1 it is necessary that

$$\Delta L_1 f_1 + \Delta L_2 f_2 = 0, \quad \Delta L_3 f_3 + \Delta L_4 f_4 = 0.$$

In addition, we will assume that

$$\max\{V(y)y \in [0,\lambda)\} - \min\{V(y)y \in [0,\lambda)\} = 1,$$

as is shown in Fig. 1, which is equivalent to fixing the value of f_1 to $f_1 = -1/\Delta L_1$. This last condition can be imposed because only the relative amplitude of $f(y)$ with respect to F_0 [the amplitude of the external forcing $F(t)$] is important to obtain nonzero current.

The above set of constraints leave us with only four free parameters in the model: three out of the four lengths $\{\Delta L_1, \Delta L_2, \Delta L_3, \Delta L_4\}$, and one of the forces $\{f_1, f_2, f_4, f_4\}$. It is more convenient to recast these four free parameters into a

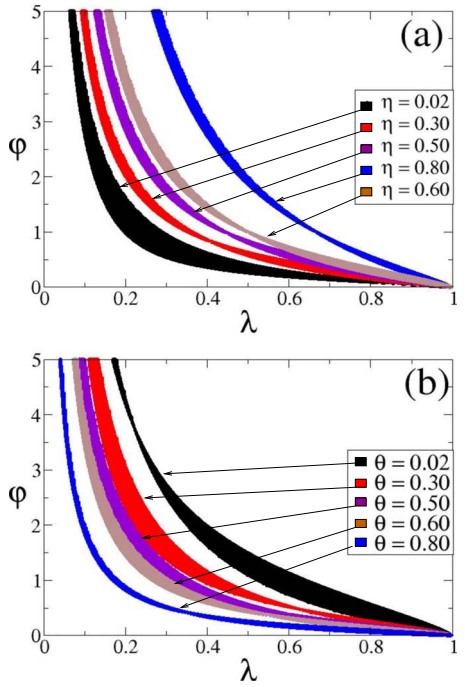

FIG. 2. (Color online) Zones of current reversals in the parameter subspace $\{\phi,\lambda\}$ for the particular ratchet potential depicted in Fig. 1 and defined by the force given in Eq. (25). The tonguelike regions where current reversals occur were calculated with the dichotomous external driving force defined in Eq. (2). (a) For $\theta=0.3$ fixed and different values of η. (b) The same as in (a) but for $\eta=0.2$ fixed and different values of θ.

different set of parameters $\{\phi,\lambda,\eta,\theta\}$ which are geometrically easy to identify [see Fig. 1(b)]. These new parameters are defined through

$$\Delta L_1 = \left(\frac{1+\eta}{2}\right)\lambda, \quad f_1 = -1/\Delta L_1, \quad \Delta L_2 = \left(\frac{1-\eta}{2}\right)\lambda,$$

$$f_2 = 1/\Delta L_2, \quad \Delta L_3 = \left(\frac{1+\theta}{2}\right)(L-\lambda),$$

$$f_3 = -\phi/\Delta L_3, \quad \Delta L_4 = \left(\frac{1-\theta}{2}\right)(L-\lambda), \quad f_4 = \phi/\Delta L_4. \tag{26}$$

Now we use the criterion given in proposition 1 to look for current reversals in the parameters space $\{\phi,\lambda,\eta,\theta\}$. The function $G(u)$ for the particular force $f(y)$ given in Eq. (25) is

$$G(u) = \sum_{i=1}^{4} \Delta L_i \sinh(u f_i), \tag{27}$$

which depends on the parameters $\{\phi,\lambda,\eta,\theta\}$ through the lengths ΔL_i and the forces f_i.

In Fig. 2 we show the zones in a subset of the parameter space for which the function $G(u)$ given in Eq. (27) exhibits changes of sign at some $u\neq 0$. Namely, the zones in the parameter space in which there is at least one current reversal

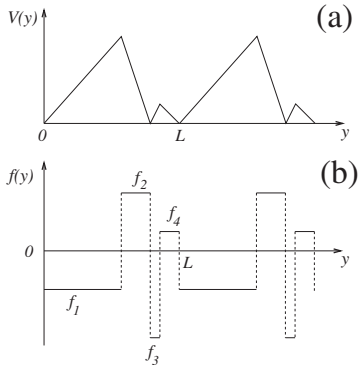

FIG. 3. (a) Ratchet potential $V(x)$ and (b) the corresponding gradient $f(y)$ exhibiting current reversals under a fully symmetric external driving force. The potential shown here is a special case of the one depicted in Fig. 1 for the following parameter values: $f_1=-5/3$, $f_2=10/3$, $f_3=-4$, $f_4=1$, $\Delta L_1=3/5$, $\Delta L_2=3/10$, $\Delta L_3=1/50$, and $\Delta L_4=4/50$ or, equivalently, for $\{\phi,\lambda,\eta,\theta\}=\{4/50,9/10,1/3,-3/5\}$.

for some forcing amplitude F_0. To generate the structures shown in Fig. 2 we fix the values of θ and η, and then explore the subspace $\{\phi,\lambda\}$ using the condition that $G(u)$ changes sign at some $u\neq 0$ to decide whether or not a point of this space exhibits current reversal. We repeat this procedure for different fixed values of θ and η. The result is the tonguelike structures shown in Fig. 2. We can think of such regions of the parameter space as those corresponding to zero rotation number for a finite value of the forcing amplitude F_0. Note that the zones of current reversal have nonvanishing area. This should be expected since it has been well established in the theory of dynamical systems [22,23] that circle maps of type we are considering here with the rational rotation number are structurally stable and hence robust. In particular, sufficiently small perturbations of the map, which can be smoothly mapped onto perturbations of the gradient of the potential, are unable to change the zero rotation number [22]. The potential $V(y)$ and the force $f(y)$ corresponding to the parameter values $\phi=4/50$, $\lambda=9/10$, $\theta=-3/5$, and $\eta=1/3$, belonging to a zone of CR of Fig. 2, are shown in Fig. 3. In our previous work we calculated numerically the current for this particular ratchet potential and exhibited [see Fig. 3(a) of Ref. [19]] that this case effectively shows a current reversal as predicted by our criterion [see Fig. 3(b) of Ref. [19]]. Notice that this effect is rather significant, i.e., a fine-tuning of the forcing amplitude F_0 is not necessary to find the current reversal.

Moreover, the amplitude of the current in both directions has the same order of magnitude, which means that even in presence of finite perturbations (noise, for example), the rectification in both directions will not be necessarily destroyed. In fact, the stability of the rational rotation number under small perturbations can be already appreciated in the steplike structure of the current as a function of the forcing amplitude. Notice also that, in order for the current to change sign, a null current should occur at a finite value of the forcing amplitude. Indeed, this vanishing current occurs along an interval of F_0 rather than just at a point, which is a consequence of the stability of the rational rotation number.

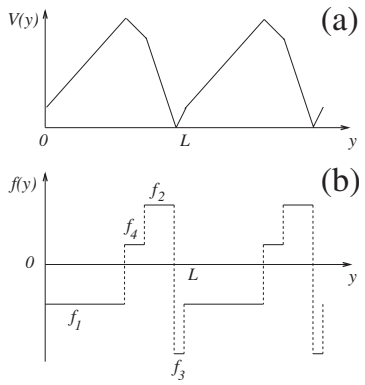

FIG. 4. (a) Potential $V(y)$ showing current reversal and (b) the corresponding force $f(y)$. Note that $f(y)$ has been generated through two permutations of the steps of $f(y)$ depicted in Fig. 3, hence $G(u)$ shown in Fig. 5(b) is the same in both cases.

Interestingly, since the sum appearing in Eq. (27) does not depend on the order in which the terms are added, given a set of parameters ΔL_i and f_i for which current reversals exist, any potential obtained by a permutation of these parameters will also lead to current reversals. For instance, Fig. 4 shows another ratchet potential that also exhibits current reversals. This new potential was obtained from the one depicted in Fig. 3 just by relocating the interval corresponding to f_4 between the intervals corresponding to f_1 and f_2. Even though the form of the potential changes, the sum in Eq. (27) does not change and therefore this potential also exhibits current reversals as is shown in Fig. 5(a). The function $G(u)$ predicting the current reversal is also presented in Fig. 5(b). This result shows that CRs can be observed in many nontrivial ratchet potentials related to each other through permutations.

We now consider a continuously differentiable potential that can be smoothly deformed by two free parameters φ and α as follows:

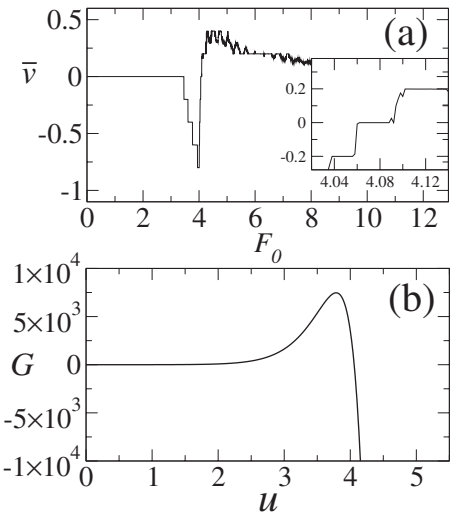

FIG. 5. (a) Mean velocity $\bar{v}$ as a function of F_0 for the step function given in Eq. (25). We have used $T=5$ for the external forcing period. The inset is an amplification. (b) Graph of $G(u)$ for the same ratchet potential. Note the change of sign in this function.

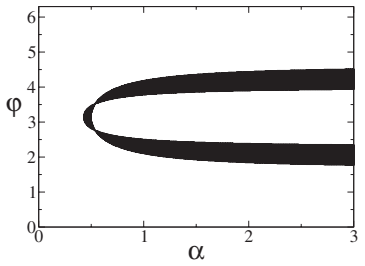

FIG. 6. Zone of current reversals in the parameter space $\{\varphi,\alpha\}$ for the potential given by Eq. (28). This zone was found by means of the criterion for current reversals that states that a current reversal will occur as a function of the forcing amplitude if the function $G(u)$ changes sign at a finite value of u.

$$V(x) = -\frac{L}{2\pi}\left(\sin(2\pi x/L) + \frac{1}{4}\sin(4\pi x/L) + \frac{\alpha}{3}\sin(6\pi x/L + \varphi)\right). \tag{28}$$

Note that this potential is actually the ratchet model introduced by Bartussek *et al.* [2] with an extra term that includes the two free parameters. The special $\alpha=0$ case reduces to Bartussek's potential. Here we again explore the parameter space $\{\varphi,\alpha\}$ using the criterion for current reversals conveyed in proposition 1 in order to establish in which regions the current reversal phenomenon takes place. In Fig. 6 we show the zone of the φ-α parameter space in which the current reversal occurs. Our span of parameters values points to a structurally stable behavior. This can be understood, as in the piecewise-linear case, in terms of the stability of the zero rotation number of the corresponding map, against perturbations of the ratchet model parameters for any finite forcing amplitude F_0.

In Fig. 7(a) we report the mean velocity $\bar{v}$ as a function of F_0 generated by the potential (28) with specific values for the parameters. The chosen values to generate this figure are $\alpha=1.0$ and $\varphi=2.3$, which fall inside the zone of current reversals presented in Fig. 6. The potential and its gradient, used to calculate the current, are presented in Fig. 7(b). Notice that the current exhibits reversals as predicted by our change of sign in $G(u)$ criterion shown in Fig. 7(c).

VI. CURRENT REVERSALS WITH CONTINUOUS FORCING

So far we have shown that the phenomenon of current reversal is widely present and robust in a variety of ratchet potentials when symmetric dichotomous forcings are used. In this section we examine two numerical examples in which current reversals are also present when the forcing is symmetric and continuous. We choose the latter as a sine function of zero mean. The first example is the piecewise-linear ratchet potential of Fig. 3, whose gradient is given by Eq. (25). The external driving force $F(t)$ that we will use in this example is

$$F(t) = F_0 \sin(2\pi t/T), \tag{29}$$

where T is the period of the external forcing.

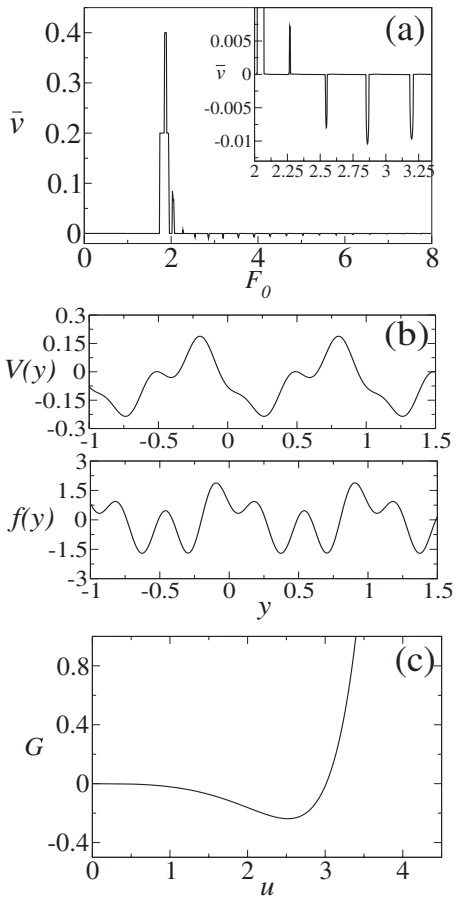

FIG. 7. Current reversals also occur for continuously differentiable potentials under dichotomous forcing. (a) The current as a function of the forcing amplitude F_0. Note that this curve exhibits the change of sign. The inset shows an amplification for a more detailed appreciation of the current reversal. (b) The potential $V(y)$ and its gradient $f(y)$ used to calculate the current in (a). Such a potential is obtained from Eq. (28) with parameter values $\alpha=1$ and $\varphi=2.3$. (c) The function $G(u)$ that predicts the existence of a CR for the potential in (b).

It is important to stress the fact that the analytic criterion for the existence of current reversals that we have derived using symmetric dichotomous forcings is not necessarily valid when $F(t)$ is continuous. This is because the quantities τ_+ and τ_- might not be well defined if $|F(t)| \leq \max|f(y)|$ for some t. In such a case it is not straightforward to convert the ratchet problem into a discrete dynamical mapping $R(x)$, although such a mapping still exists. However, from Fig. 8 which shows for the model described by Eqs. (25) and (29) the current as a function of the forcing amplitude F_0 for a fixed period of $T=5$, it is apparent that current reversals do occur. Moreover, since the currents in both directions are of the same order of magnitude, this current reversal is not a negligible effect. It is also important to remark that, though we observed current reversals for both, dichotomous and continuous sine forcings, the preservation of the CRs under a discrete to continuous transformation does not always hold, even for symmetry preserving cases. We have found counterexamples where a ratchet potential that exhibits current reversal under dichotomous forcing, no longer presents such a phenomenon under the sine continuous forcing.

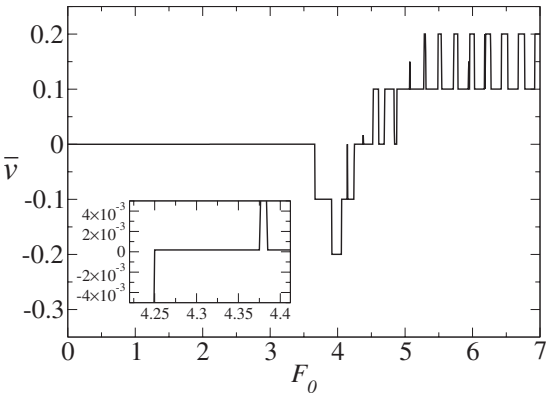

FIG. 8. Current reversal for continuous forcing. We use the external forcing given in Eq. (29) and the ratchet potential depicted in Fig. 3. Notice that the order of magnitude of the current in both direction is the same. The origin of the "plateau" structure (or "current quantization") can be explained in terms of the rational rotation number stability of the associated circle map. In particular, this implies that the zero current behavior in the transition from negative to positive flux is structurally stable (it occurs along an interval rather than just at a point, as shown in the inset). Hence, the current reversal should be robust under small changes in the potential.

Another peculiar behavior is the occurrence of the "plateau" structures, which were previously described in Refs. [2,7] and linked to devil staircases and phase-locking phenomena. Here, we consider these structures as a signature of the robustness of current reversals that we have seen using discontinuous dichotomous forcings. In other words, we argue that the stability of rational rotation numbers under perturbations of the model parameters gives rise to the "quantization" of the ratchet current when the amplitude of the external forcing is changed. The above would imply that the null current (zero rotation number) behavior arising from the negative to positive flux transition in the J-vs-F_0 curve is also structurally stable. Thus, we expect small changes in the potential to be unable to inhibit this effect, rendering a robust behavior for the current reversals.

The second example that we analyze with the continuous forcing $F(t)$ given in Eq. (29) also involves a continuously differentiable ratchet potential $V(y)$. This potential was obtained by retaining in the Fourier series of the potential shown in Fig. 3 the first 32 terms. In this case, the system also exhibits current reversals when F_0 is varied, as it is shown in Fig. 9. The period of the forcing $F(t)$ used to generate this figure is $T=10$. It is apparent from Fig. 9 that the current vs forcing amplitude curve also has a plateau structure, which reveals the stability of the current reversal under changes in the potential. Actually, such a stability is expected in this case since by adding successive terms to the truncated Fourier series we slowly modify the ratchet profile. However, the current reversal does not disappear as it was already shown for the original piecewise linear potential of Fig. 3.

VII. CONCLUSIONS

In this paper we have shown that current reversals in deterministic overdamped tilting ratchets under symmetric

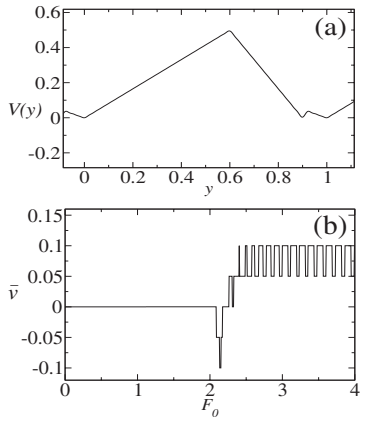

FIG. 9. Current reversal for the continuous forcing given in Eq. (29) and with a continuously differentiable potential. (a) The smooth potential obtained from the Fourier series of Eq. (25) by retaining the first 32 terms of the original ratchet potential depicted in Fig. 3. (b) The current as a function of the forcing amplitude. Notice that the order of magnitude of the current in both directions is the same and that the plateau structures are also present in this case. The period of the external forcing is $T=10$.

driving forces are not negligible and robust. This has been done through the formalism introduced by the authors in Ref. [19] and the analytical criterion given therein. We have explained in more detail, and extended to more general cases, our previous results related to the link between deterministic ratchets and circle maps. We have introduced several numerical examples that illustrate our claims. In particular, we have analyzed the relation of the robustness of current reversals to the structural stability, associated with rational rotation numbers, under small changes in the model parameters. This was done through the identification of the zones of current reversal in the parameter space with the zones of null rotation number for a nonzero value of the forcing amplitude, namely, the Arnold tongues with to zero rotation number. We have also presented two numerical examples in which current reversals are observed with a continuous external forcing. For these cases, the plateau structure of the current as a function of the forcing amplitude can be understood as a direct consequence of the structural stability for rational rotation number. These considerations suggest that, current reversals in ratchet systems are robust and not uncommon under arbitrary symmetric continuous forcings, a characteristic of overdamped tilting ratchets that, which to our knowledge has not been previously stated.

ACKNOWLEDGMENTS

This work was supported by CONACyT Grant No. P47836-F and by PAPIIT-UNAM Grant No. IN112407-3. R. S.-G. acknowledges CONACyT for support.

APPENDIX A: INVARIANCE OF $\dot{y}=f(y)+F(t)$ UNDER L,T SHIFTS

Here we prove properties I and II which provide the link between deterministic ratchets and circle maps. We start with property I. Let $Y(t;y_0)$ be the general solution of the differential equation

$$\dot{y} = f(y) + F(t), \tag{A1}$$

with the initial condition $y(0)=y_0$. We define $u(t)$ as $u(t)=y(t)+L$. From the periodicity of $f(y)$, it follows that $u(t)$ satisfies the differential equation

$$\dot{u} = f(u) + F(t). \tag{A2}$$

Considering the initial value problem $u(0)=y_0+L$, the general solution can be written as

$$u(t) = Y(t;y_0 + L),$$

since Eqs. (A2) and (A1) are equivalent. Going back from the variable u to y, the last expression can be written as

$$y(t) + L = Y(t;y_0 + L). \tag{A3}$$

Note that, since $u(t)$ has the value y_0+L at $t=0$, then $y(t)=u(t)-L$ takes the value y_0 at $t=0$. Therefore $y(t)$ can be written as $y(t)=Y(t;y_0)$, which, together with Eq. (A3) implies that

$$Y(t;y_0) + L = Y(t;y_0 + L), \tag{A4}$$

which is the property I

The proof of the property II is as follows. Consider Eq. (A1) with the initial value problem $y(0)=y_1$. The solution can be written as

$$y(t) = Y(t;y_1). \tag{A5}$$

Now, let τ be a shifted time variable $\tau=t+T$. Then, y as function of τ, satisfies the differential equation,

$$\frac{d\tilde{y}}{d\tau} = f(\tilde{y}) + F(\tau),$$

where we have defined $\tilde{y}(\tau)=y(\tau-T)=y(t)$, and used the fact that $F(t)$ is periodic with period T. For the initial value problem $\tilde{y}(0)=y_0$ it is clear that

$$\tilde{y}(\tau) = Y(\tau;y_0), \tag{A6}$$

which, in terms of t and y becomes

$$y(t) = Y(t + T;y_0). \tag{A7}$$

From the last equation, we see that $y(t)$ takes the value $y(0)=Y(T;y_0)$ at $t=0$. If we take $y_1=Y(T;y_0)$ in Eq. (A5), then

$$y(t) = Y[t;Y(T;y_0)],$$

which, together with Eq. (A7) implies

$$Y[t;Y(T;y_0)] = Y(t + T;y_0),$$

which is property II.

APPENDIX B: DETERMINISTIC RATCHETS AS CIRCLE MAPS

Here we prove that, if properties I and II hold, then the function R_T satisfies the following. (i) R_T is a monotonically

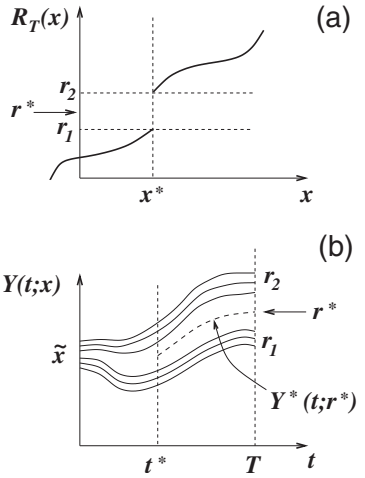

FIG. 10. (a) A jump discontinuity in R_T. If such a discontinuity occurs at some x^* we see that R_T cannot take values in the interval (r_1,r_2), i.e., there is no $x \in \mathbb{R}$ such that $R_T(x)=r^*$ for $r^* \in [r_1,r_2)$. (b) The jump discontinuity implies either that the uniqueness of the solution $Y(t;x)$ does not hold at $t=0$ (or at some $t^*>0$), or that some solutions are missing, which contradicts existence. Thus, the jump discontinuity cannot occur.

increasing function with continuous inverse. (ii) R_T satisfies the lift property, i.e., $R_T(x+L)=R_T(x)+L$. (iii) R_T satisfies the group property, i.e., $R_T \circ R_T = R_{2T}$.

The proof is as follows. Property (i) is a consequence of the existence and uniqueness theorem of the solutions of Eq. (1). Let $y_1(t)$ and $y_2(t)$ be two different solutions of Eq. (A1), and assume that $y_1(t_0)>y_2(t_0)$ for some t_0. Due to the fact that the solutions $y_1(t)$ and $y_2(t)$ cannot cross each other, then it must happen that $y_1(t)>y_2(t)$ for all t. Therefore, if $x_0=y_1(0)$, $x_0'=y_2(0)$, $x_1=y_1(T)$, and $x_1'=y_2(T)$ such that $x_0>x_0'$, then $x_1>x_1'$. Since $x_1=R_T(x_0)$ and $x_1'=R_T(x_0')$, the above argument shows that if $x_0>x_0'$ then $R_T(x_0)>R_T(x_0')$, which implies that $R(x)$ is a monotonically increasing function.

To show that R_T is continuous we take into account two possible scenarios in which continuity can be violated. These are (a) a divergent discontinuity at finite x and (b) a jump discontinuity. Discontinuities of type (a) cannot occur due to the fact that $R_T(x)-x$ is bounded for all x. This can be seen if we rewrite down the formal solution of Eq. (1) as

$$Y(T;y_0) = y_0 + \int_0^T \{f[Y(t;y_0)] + F(t)\}dt.$$

Since both $f(y)$ and $F(t)$ are bounded it follows that $Y(T;y_0)-y_0$ is also bounded for all y_0, from which it follows that $R_T(x)-x$ cannot diverge.

To show that divergences of type (b) do not take place we invoke the existence and uniqueness theorem. Let us assume that $R_T(x)$ has a discontinuity at some x^* such that $\lim_{x\to x^{*-}} R_T(x)=r_1$ and $\lim_{x\to x^{*+}} R_T(x)=r_2$ [see Fig. 10(a)]. Then, for some $r^* \in (r_1,r_2)$ there does not exist $x \in \mathbb{R}$ with $R_T(x)=Y(T;x)=r^*$. However, due to the existence theorem, the initial value problem $y(T)=r^*$ for the differential Eq. (1) should have a unique solution $Y^*(t;r^*)$. Moreover, since this particular $Y^*(t;r^*)$ should also be defined for all $t \in \mathbb{R}$, then, there must exist a $\tilde{x} \in \mathbb{R}$ such that $Y^*(0;r^*)=\tilde{x}$. This contradicts the initial statement that such an $\tilde{x}$ does not exist [see Fig. 10(b)]. Therefore, $R_T(x)$ does not have jumps in $\mathbb{R}$. Since $R_T(x)$ is continuous and monotonically increasing, it has a well defined continuous inverse.

Properties (ii) and (iii) can be proved directly by writing $R_T(x)=Y(T;x)$ and applying the properties I and II, already proven, to $Y(T;x)$. Finally it should be noted that, by property (iii), the iteration of the map $R_T(x)$ with initial condition $x_0=y_0$, produces a sequence $\{x_0,x_1,x_2,\ldots,x_n,\ldots\}$, with $x_n=R_T(x_{n-1})$ that can be identified as the periodic (with period T) stroboscopic sampling of the solution $y(t)$ of Eq. (1) with the initial condition $Y(0)=y_0$. Furthermore, due to properties (i) and (ii), $R_T(x)$ can be interpreted as a lift of an invertible circle homeomorphism [22]. This establishes the formal link between deterministic ratchets and circle maps.

APPENDIX C: PROOF OF THE NULL CURRENT CONDITION

In Ref. [19] we have shown that the current is zero if and only if the gradient of the potential satisfies the condition given in Eq. (21). In that proof we explicitly assumed that the forcing amplitude F_0 is larger than $\max\{|f(y)|\}$. Here we show that the last restriction is not necessary and that the validity of Eq. (21) holds true for the entire parameter space $\{F_0,T\}$.

First let us prove that if the null current condition given in Eq. (21) is satisfied by some $f(y)$, then $\max\{f(y)\}=|\min\{f(y)\}|$. Since the condition of zero current is equivalent to $\tau_+(F_0)=-\tau_-(F_0)$ [see Eq. (22) and Ref. [19]], then $f(y)$ should satisfy

$$\int_0^L \frac{dx}{f(y)+F_0} = -\int_0^L \frac{dx}{f(y)-F_0}, \tag{C1}$$

for every $F_0>\max|f(y)|$. We now show that the assumption $\max\{f(y)\}>|\min\{f(y)\}|$ leads to a contradiction. It is convenient to define the quantities f_- and f_+ as

$$f_- = \max\{f(y)\}, \tag{C2}$$

$$f_+ = |\min\{f(y)\}|.$$

With the above definitions, it follows from Eqs. (6a) and (10a) that

$$\lim_{F_0\to f_+} \tau_+(F_0) = \infty, \tag{C3}$$

$$\lim_{F_0\to f_-} \tau_-(F_0) = -\infty. \tag{C4}$$

Then, for every $M>0$ there is an ε such that

$$|\tau_-(f_- + \epsilon)| > M.$$

On the other hand, if $F_0=f_-$ then $\tau_+(F_0)$ is well defined since, by hypothesis, $f_->f_+$. Hence, there is a value $\tilde{M}>0$ such that (see Fig. 11)

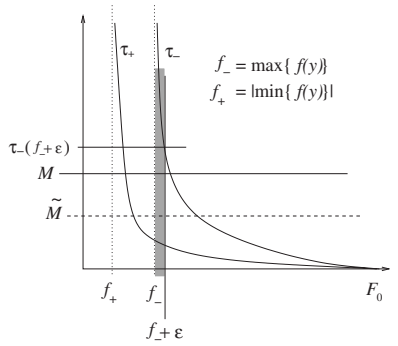

FIG. 11. The functions $\tau_+(F_0)$ and $|\tau_-(F_0)|$ for $f_->f_+$. It is easy to see that in this case it is impossible for $\tau_+(F_0)=-\tau_-(F_0)$ to hold for every $F_0>f_-$ due to the fact that the divergences of these quantities take place at different values of F_0. As it is explained in the text, the proof is based on the fact that for any small $\epsilon>0$, $|\tau_-(f_-+\epsilon)|$ is larger that $\tau_+(f_-+\epsilon)$. Establishing a lower bound for τ_- and an upper bound for τ_+ we guarantee the existence of an $\tilde{F}$ between f_- and $f_-+\epsilon$ (the shaded zone in the figure) such that $\tau_+(\tilde{F})<|\tau_-(\tilde{F})|$ which contradicts the initial statement $\tau_+(F_0)=-\tau_-(F_0)$.

$$\tau_+(f_-)<\tilde{M}.$$

Moreover, since $\tau_+(F_0)$ is a decreasing function of F_0, then the inequality $\tau_+(F_0)<\tilde{M}$ holds for every $F_0>f_-$. The choice $M>\tilde{M}$ guarantees the existence of an $\tilde{\epsilon}\in(0,\epsilon]$ such that if $\tilde{F}=f_-+\tilde{\epsilon}$ then

$$\tau_+(\tilde{F})<|\tau_-(\tilde{F})|$$

holds (see Fig. 11), which contradicts the initial statement (C1).

A similar argument shows that the assumption $f_+>f_-$ also leads to a contradiction. Therefore, we can say that whenever a function $f(y)$ fulfills Eq. (21) it necessarily satisfies that $f_-=f_+\equiv F_c$. In Appendix E we prove that for $F_0=F_c$ the current is zero due to the fact that $R_T=M_-\circ M_+$ has fixed points.

Actually, the above condition on F_0 for the existence of fixed points for R_T can be extended to $F_0<F_c$. Here we only outline the proof of this result by means of geometrical arguments. We have identified the fixed points $M_\pm$ with the roots of $f(y)\pm F_0$. Moreover, the stability of such fixed points, as well as the order in which they are located along $\mathbb{R}$, can be inferred from the sketch of the functions $f(y)+F_0$ and $f(y)-F_0$ shown in Fig. 12(a). Note that the fixed point equation $R_T(x)=x$ can be written as $M_-(x)-M_+^{(-1)}(x)=0$. If we sketch the maps $M_-(x)$ and $M_+^{(-1)}(x)$ [see Fig. 12(b)] the fixed point information is enough to prove, along the same line of reasoning as in Appendix E, that $M_-(x)-M_+^{(-1)}(x)=0$ always has a solution. But before showing this, we need to prove another intermediate property related to circle homeomorphisms.

APPENDIX D: SOME PROPERTIES OF LIFTS OF CIRCLE HOMEOMORPHISMS

Here we show that if $h(x)$ is a lift of a circle homeomorphism, then the function $g(x)=h(x)-x$ is periodic, with period L, and with a bounded amplitude such that $|g(x)-g(y)|<L\,\forall\,x,y\in\mathbb{R}$. A lift of an invertible circle homeomorphism h satisfies the following two properties:

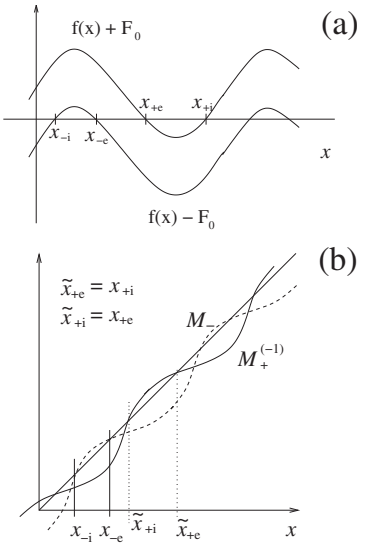

FIG. 12. (a) Net forces acting on the particle every half period. The plots of these net forces $f(y)+F_0$ and $f(y)-F_0$ give information about the location and the stability of the fixed points of the associated maps M_+ and M_-, respectively. (b) The maps $M_\pm$. With the information about the fixed points inferred from (a) we can sketch the maps $M_+^{(-1)}$ and M_- (recall that the inverse of a function inverts the stability of the fixed point but retains its location). Note the order of the fixed points is important for say that $M_-(x)=M_+^{(-1)}(x)$ to always have solutions.

$$h(x)>h(y) \quad \text{if and only if} \quad x>y, \tag{D1}$$

$$h(x+L)=h(x)+L. \tag{D2}$$

Property (D2) implies that $g(x+L)=h(x+L)-(x+L)=h(x)-x=g(x)$, from which the periodicity of g follows.

Let $x,y\in\mathbb{R}$ be two real numbers such that $0<x-y<L$. Note that property (D1) ensures that

$$0<h(x)-h(y). \tag{D3}$$

Moreover, let $\delta=x-y<L$ be a positive number, then by monotonicity

$$h(x)=h(y+\delta)<h(y+L),$$

and therefore $h(x)<h(y)+L$. This result, together with (D3), leads to

$$0<h(x)-h(y)<L. \tag{D4}$$

Now note that the last statement implies that

$$h(x)-h(y)-(x-y)>-(x-y)>-L$$

and

$$h(x)-h(y)-(x-y)<L-(x-y)<L.$$

Therefore,

$$-L < h(x) - h(y) - (x-y) < L$$

or, in terms of g,

$$|g(x) - g(y)| < L. \tag{D5}$$

The above expression remains valid for any $x, y \in \mathbb{R}$ due to the periodicity of g. We will say that g is a function of bounded amplitude if it satisfies Eq. (D5).

It should be noted that, since $h^{(-1)}(x)$ is also a lift of a circle homeomorphism, it can also be written as $h^{(-1)}(x)=x+\bar{g}(x)$, where $\bar{g}(x)$ is a function of bounded amplitude and periodic with period L. Now set $x=h^{(-1)}(y)$, then,

$$h(x) = x + g(x) = h^{(-1)}(y) + g(x) = y + \bar{g}(y) + g(x), \tag{D6}$$

from which it follows that

$$g(x) = -\bar{g}[h(x)]. \tag{D7}$$

APPENDIX E: NULL CURRENT AT $F_0=F_c$

Now, let us go back to the problem of showing that if $f_-=f_+\equiv F_c$, then the map $R_T(x)=(M_-\circ M_+)(x)$ has fixed points at $F_0=F_c$, where f_- and f_+ are defined as in Eq. (C2). Recall that the fixed points of the maps M_+ and M_- occur at the roots of $f(y)+F_0=0$ and $f(y)-F_0=0$, respectively. For $F_0=F_c$ these functions satisfy

$$f(y) + F_0 \geq 0, \tag{E1}$$

$$f(y) - F_0 \leq 0. \tag{E2}$$

We will assume, without loss of generality, that the equality holds only once per period, which means that $f(y)$ has only one absolute maximum and one absolute minimum per period.

The maps M_+ and M_- are defined from the solutions of the differential equations

$$\frac{dy_+}{dt} = f(y_+) + F_0 \tag{E3}$$

and

$$\frac{dy_-}{dt} = f(y_-) - F_0, \tag{E4}$$

as $M_+(x)=Y_+(T;x)$ and $M_-(x)=Y_-(T;x)$, where Y_+ and Y_- are the general solutions to Eqs. (E3) and (E4), respectively, with the initial condition $y_\pm(0)=x$. Thus, by the inequalities (E1) and (E2) we have that

$$g_+(x) \equiv M_+(x) - x = \int_0^T \{f[y_+(t)] + F_0\} dt \geq 0$$

and

$$g_-(x) \equiv M_-(x) - x = \int_0^T \{f[y_-(t)] - F_0\} dt \leq 0.$$

The above means that, while the positive pulse $+F_0$ is acting, the particle either goes forward or it gets stuck. Analogously, when the negative pulse $-F_0$ is acting the particle goes backward or it gets stuck.

Note that the fixed point equation $R_T(x)=(M_-\circ M_+)(x)=x$ is equivalent to $M_+(x)=M_-^{(-1)}(x)$. Defining the function $\bar{g}(x)=M_-^{(-1)}(x)-x$, the fixed point equation $R_T(x)=x$ can be written as

$$g_+(x) = \bar{g}_-(x).$$

Using the result given in Eq. (D7) we obtain

$$g_+(x) + g_-[M_-^{(-1)}(x)] = 0. \tag{E5}$$

To show that there exists a point $x=\xi$ for which the above equation is satisfied, we evaluate the quantity $g_+(x)+g_-[M_-^{(-1)}(x)]$ at the fixed point of M_+, which we call ξ_+ and is unique per period. We then obtain

$$g_+(\xi_+) + g_-[M_-^{(-1)}(\xi_+)] = g_-[M_-^{(-1)}(\xi_+)] < 0, \tag{E6}$$

where we have used the fact that $g_+(\xi_+)=M_+(\xi_+)-\xi_+=0$. On the other hand, by evaluating Eq. (E5) at the fixed point of M_-, which we call ξ_-, it is clear that

$$g_+(\xi_-) + g_-[M_-^{(-1)}(\xi_-)] = g_+(\xi_-) > 0, \tag{E7}$$

Therefore, by the mean value theorem and by the continuity of the functions M_+ and M_-, there must exist a $\xi \in [\xi_-, \xi_+]$ such that $g_+(\xi)+g_-[M_-^{(-1)}(\xi)]=0$, which is equivalent to $R_T(\xi)=\xi$.

APPENDIX F: CURRENT REVERSALS AT THE ADIABATIC LIMIT

Here we give a proof of proposition I by means of asymptotic expressions for the Laplace transform of $G(u)$. This quantity is related to the mean velocity at the adiabatic limit $\bar{v}_\infty$ through $\tau_+-\tau_-$ as is stated by Eqs. (22) and (24). Thus we write

$$\bar{v}_\infty = -\frac{L}{\tau_+\tau_-} H(F), \tag{F1}$$

where $H(F)$ is defined as the Laplace transform of $G(u)$,

$$H(F) := \int_0^\infty e^{-uF} G(u) du. \tag{F2}$$

To prove proposition I, we only need to prove that if $G(u)$ changes sign at a unique $u^* \neq 0$ then $H(F)$ also changes sign at some $F^* \neq 0$.

Let $P(F)$ and $N(F)$ be defined by

$$P(F) := \int_0^{u^*} e^{-uF} G(u) du, \tag{F3}$$

$$N(F) := \int_{u^*}^\infty e^{-uF} G(u) du. \tag{F4}$$

Note the $H=P+N$ and that $\text{sign}(P)=-\text{sign}(N)$ for each $F > F_c := \max\{|f(x)|\}$. This is true under the assumption that $G(u)$ changes sign only once in all $\mathbb{R}^+$. Now we calculate

asymptotic expressions for P and N in two limiting cases (i) $F_0 \to \infty$ and (ii) $F_0 \to F_c$.

Case (i). If $F \to \infty$ we can easily check that

$$P(F) \approx \frac{G'''(0)}{F^4}, \tag{F5}$$

since the first nonvanishing term in the Taylor expansion of G is $G'''(0)u^3/3!$ [25]. The error introduced in Eq. (F5) should necessarily vanish faster than F^{-4}. So, without loss of generality, the remainder in the truncated expansion of P can be bounded, for large F, by $C_p F^{-5}$ where $C_p > 0$ is an appropriate constant. Thus we have

$$-\frac{C_p}{F^5} \leq |P(F)| - \left|\frac{G'''(0)}{F^4}\right| \leq \frac{C_p}{F^5}. \tag{F6}$$

In a similar way, for $N(F)$ we can write

$$-\frac{C_n e^{-u^* F}}{F^3} \leq |N(F)| - \left|\frac{G'(u^*)e^{-u^* F}}{F^2}\right| \leq \frac{C_n e^{-u^* F}}{F^3} \tag{F7}$$

since the leading order in the expansion of N is $F^{-2}e^{-u^* F}$ for F large enough. As in the case of $P(F)$, we assume that the remainder in the asymptotic expansion of N can be bounded by a constant C_n times a function of a lower order than the order of the leading term. Thus, inequalities (F6) and (F7) imply that there exists an $\tilde{F}$ (large enough) such that for all $F > \tilde{F}$, the following inequality holds:

$$|P(F) > |N(F)|. \tag{F8}$$

Case (ii). If $F \to F_c$ we should note that $P(F) \to K_p$ where K_p is a constant (independent of F) given by

$$K_p := \int_0^{u^*} G(u)e^{-uF_c}du.$$

Moreover, since

$$|P(F+\Delta F)| = \left|\int_0^{u^*} G(u)e^{-uF}e^{-u\Delta F}du\right| < \left|\int_0^{u^*} G(u)e^{-uF}du\right| = |P(F)|,$$

which is true because $e^{-u\Delta F} < 1$ for all $u > 0$, we have that $|K_p|$ is an upper bound for $|P(F)|$,

$$|P(F)| \leq |K_p|. \tag{F9}$$

On the other hand, from the following argument, we have that $N(F)$ diverges as F goes to F_c. Since P is bounded it suffices to show that $H=N+P$ diverges itself. Notice also that,

$$H(F) = -\frac{1}{2}[\tau_+(F) + \tau_-(F)], \tag{F10}$$

where τ_+ and τ_- were defined as

$$\tau_+(F) = \int_0^L \frac{dx}{f(x)+F}, \quad \tau_-(F) = \int_0^L \frac{dx}{f(x)-F}.$$

The assumption that $\max\{f(x)\} \neq |\min\{f(x)\}|$, from which follows the asymmetry of $V(x)$, implies that either, τ_+ or τ_- diverges at $F=F_c$. We thus have that $H(F)$ indeed diverges and therefore $|N(F)|$ has no finite upper bound. Thus, by virtue of Eq. (F9) there exists an $\epsilon > 0$ (small enough) such that for all $F \in (F_c, F_c+\epsilon)$ the following inequality holds:

$$|P(F)| < |N(F)|. \tag{F11}$$

Finally, inequality (F8) together with Eq. (F11) imply that there is an F^* where $H(F^*)=0$ and a change of sign takes place. This completes the proof of proposition I.

[1] P. Reimann, Phys. Rep. **361**, 57 (2002).
[2] R. Bartussek, P. Hänggi, and J. K. Kissner, Europhys. Lett. **28**, 459 (1994).
[3] P. Jung, J. G. Kissner, and P. Hänggi, Phys. Rev. Lett. **76**, 3436 (1996).
[4] J. L. Mateos, Phys. Rev. Lett. **84**, 258 (2000).
[5] M. Barbi and M. Salerno, Phys. Rev. E **62**, 1988 (2000).
[6] J. L. Mateos, Physica A **325**, 92 (2003).
[7] A. Ajdari, D. Mukamel, L. Peliti, and J. Prost, J. Phys. I **4**, 1551 (1994).
[8] A. Sarmiento and H. Larralde, Phys. Rev. E **59**, 4878 (1999).
[9] M. M. Millonas and M. I. Dykman, Phys. Lett. A **185**, 65 (1994).
[10] J. Kula, M. Kostur, and J. Luczka, Chem. Phys. **235**, 27 (1998).
[11] R. Mankin, A. Ainsaar, and E. Reiter, Phys. Rev. E **61**, 6359 (2000).
[12] M. Arrayás, R. Mannella, P. V. E. McClintock, A. J. McKane, and N. D. Stein, Phys. Rev. E **61**, 139 (2000).
[13] M. Kostur and J. Luczka, Phys. Rev. E **63**, 021101 (2001).
[14] I. Derényi and T. Vicsek, Phys. Rev. Lett. **75**, 374 (1995).
[15] Z. Csahók, F. Family, and T. Vicsek, Phys. Rev. E **55**, 5179 (1997).
[16] G. Cocho, A. Cruz, G. Martínez-Mekler, and R. Salgado-García, Physica A **327**, 151 (2003).
[17] M. O. Magnasco, Phys. Rev. Lett. **71**, 1477 (1993).
[18] M. Schreier, P. Reimann, P. Hänggi, and E. Pollak, Europhys. Lett. **44**, 416 (1998).
[19] R. Salgado-García, M. Aldana, and G. Martínez-Mekler, Phys. Rev. Lett. **96**, 134101 (2006).
[20] S. Flach, O. Yevtushenko, and Y. Zolotaryuk, Phys. Rev. Lett. **84**, 2358 (2000).
[21] P. Reimann, Phys. Rev. Lett. **86**, 4992 (2001).
[22] B. Hasselblatt and A. Katok, *A First Course in Dynamics* (Cambridge University Press, Cambridge, 2003).
[23] V. I. Arnold, *Geometrical Methods in the Theory of Ordinary*

Differential Equations (Springer Verlag, New York, 1988).
[24] The proof for the case of multiple roots is a straightforward generalization of Appendix F.
[25] The order of the first nonvanishing term can be larger than 3. However, for the sake of clarity, in the proof we assume that the Taylor series starts with the third derivative term since the first three terms are strictly zero. The arguments of the proof can easily be generalized if this is not the case.